

# Controlled Decomposable Hydrogel Triggered with a Specific Enzyme

You-Ren Ji,<sup>¶</sup> Ya-Hsiang Hsu,<sup>¶</sup> Ming-Hua Syue, Ying-Chu Wang, Shyr-Yi Lin,<sup>\*</sup> Tsung-Wei Huang,<sup>\*</sup> and Tai-Horng Young<sup>\*</sup>



Cite This: *ACS Omega* 2022, 7, 3254–3261



Read Online

ACCESS |



Metrics & More

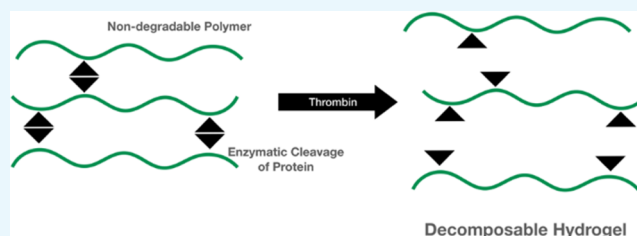


Article Recommendations



Supporting Information

**ABSTRACT:** In this study, superabsorbent polyelectrolyte hydrogels were synthesized by cross-linking a nondegradable poly(allylamine hydrochloride) (PAH) and a recombinant protein with a specific enzymatic cleavage site. The recombinant protein was produced by *E. coli* with the pET-32b(+) plasmid, which is featured with the thioredoxin (Trx) gene containing a thrombin recognition site and a T7/lac hybrid promoter for high expression of recombinant protein. The swelling test shows that the composite hydrogel still maintained a high swelling ratio to 900% when 15% recombinant protein was cross-linked with PAH. The degradation test shows that such a PAH composite hydrogel could be decomposed by the addition of specific enzyme thrombin, which might lead to new biomedical applications of hydrogels needed to be decomposable by specific time not determined by the time period.



## INTRODUCTION

The development of biodegradable polymers has attracted considerable interest for a variety of applications, such as implants, drug delivery, and tissue engineering in the past decades.<sup>1–5</sup> These biomaterials degrade with controllable kinetics and low toxic products. The degradation type of biomaterials can be mainly categorized into hydrolytic and enzymatic degradation.<sup>6</sup> A hydrolytic degradation rate is generally controlled by the properties of the materials, such as molecular weight, crystallinity, hydrophilicity, roughness, and so on.<sup>7,8</sup> Generally, the mechanical property of hydrolytically degradable biomaterials is constantly changing with time, so more precisely controlled degradable biomaterials need an optimum balance between mechanical properties and degradation rate. Conversely, in enzymatic degradation, materials were developed to incorporate cleavage sites for enzymes, so the degradation is determined by the presence of enzyme and its activity rather than implantation time.<sup>9</sup>

Polyallylamine hydrochloride (PAH) is a nondegradable polyelectrolyte and is widely used in biomedical research as a positively charged and amino-rich polymer.<sup>10–12</sup> Thus, PAH is extensively applied to prepare superabsorbent hydrogels, which can absorb tremendously large amounts of water.<sup>13</sup> The aim of this study is to modify the PAH hydrogel structure with a recombinant protein, which possesses a specific enzymatic cleavage site. The recombinant protein in this study was produced by *E. coli* with the pET-32b(+) plasmid.<sup>14</sup> The pET system plasmid has been designed for cloning and expression of proteins in *E. coli*. The pET-32b(+) plasmid is featured with the thioredoxin (Trx) gene containing a thrombin recognition

site and a T7/lac hybrid promoter for high expression of recombinant protein. Therefore, the superabsorbent PAH cross-linked with the recombinant protein with a specific enzymatic cleavage site can be decomposed by additional specific enzymes at the indicated time point, which might lead to new biomedical applications of hydrogels needed to be decomposable by specific time not determined by the time period.

## RESULTS

**Characterization of the pET-32b(+) Plasmid.** In this study, the pET-32b(+) plasmid is designed with a T7/lac hybrid promoter for high expression of recombinant protein and is featured with a thrombin recognition site. The pET-32b(+) is a 5899 bp plasmid extracted from *E. coli* cloning cells (ECOS) and transferred into *E. coli* BL21 for protein expression. Figure 1 shows that both plasmids extracted from ECOS and *E. coli* BL21 and digested by BamHI restriction enzymes would exhibit similar bands at about 5900 bps by agarose gel electrophoresis analysis.

**Characterization of TP.** After transferring the pET32b (+) into the *E. coli* BL21, the TP with a molecular weight of 20 kDa was expressed. The SDS-PAGE analyses revealed that the

Received: September 17, 2021

Accepted: January 12, 2022

Published: January 21, 2022



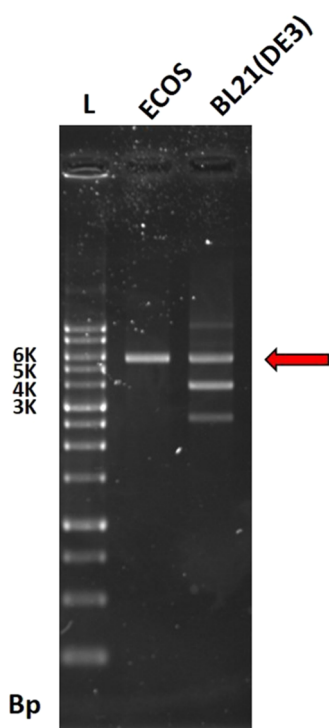


**Figure 1.** Agarose gel electrophoresis analysis of the pET-32b(+) plasmid extracted from ECOS and BL21 after transforming (Bp: bonding pair, L: DNA ladder; E: pET-32b(+) plasmid from ECOS cleaved by BamHI; and B: pET-32b(+) plasmid from BL21 cleaved by BamHI).

TP expression after culture for 10 h was higher in the IPTG-induced group than in the control without induction (Figure 2). Additionally, the TP expression increased as the culture time increased and reached the plateau in 8–10 h. Therefore, further experiments to yield the TP were performed with an IPTG induction time of 10 h.

**Purification of TP.** Bacterial components were separated into the supernatant and pellet after disrupting and centrifuging the bacteria. To choose an appropriate purification process, the water solubility of TP was evaluated in advance. Figure 3A shows that 20 KDa TP occurred more in the supernatant than in the pellet, so the supernatant product was employed in the following purification process. SDS-PAGE

analyses confirmed that TP was effectively trapped by the HisTrap column and no expression of TP was found in binding buffer and wash buffer (Figure 3B) since TP with a hexahistidine tag at the N-terminal could be purified with HisTrap columns. Furthermore, the elution buffer passed through the purification column revealed significant expression of TP in the first two volumes and extremely low expression in the last two volumes. These results indicated that the TP was successfully purified from the hybrid protein solution and effectively collected from the HisTrap column.

**Cleavage Test.** The SDS-PAGE analyses shown in Figure 4 revealed that TP would not be cleaved while the concentration of thrombin was lower than  $2.5 \times 10^{-3}$  U/mL. In contrast, thrombin could specifically cleave the TP into two fractions with a size of 14 and 6 kDa, respectively, with the concentration of thrombin more than  $2.5 \times 10^{-2}$  U/mL.

**Formation and FTIR Analysis of the PAH Composite Hydrogel.** To design novel enzyme-triggered degradable biomaterials, PAH and the synthesized protein were cross-linked by the reaction of glutaraldehyde with amino groups of protein and PAH (Figure 5A). Since the solution with 5% PAH was unable to form gel and the 20% TP concentration could not form homogeneous hydrogels with PAH, the hydrogels were formed by hybridizing 10% PAH with 5, 10, and 15% protein, as shown in Figure 5B by the inversion test. All gels were characterized using FTIR, and all main peaks are shown in Figures S-1 and 6C. Compared to PAH without cross-linking (Figure S-1), the FTIR spectrum of PAH gel is shifted from  $1633 \text{ cm}^{-1}$  (N–H scissor vibrations) to  $1604 \text{ cm}^{-1}$  (C=N stretching), confirming that 10P was prepared by glutaraldehyde cross-linking. On the other hand, compared to 10P-only (Figure 5C), the FTIR spectrum of PAH composite gels included a C–O stretching characteristic peak at  $1053 \text{ cm}^{-1}$ , and the peak increased with the increase in protein content, which assured the aldehyde cross-linking reaction.

**Swelling Test of the PAH Composite Hydrogel.** The swelling ratio is a significant characteristic of PAH, determining the application of hydrogel materials. Figure 6 shows the swelling kinetics of the composite hydrogels incubated in TBS buffer. The PAH hydrogel without protein has the highest swelling ratio to 30-fold within 2 h. The higher ratio of protein contained in the PAH composite hydrogel indicated the lower swelling ratio. The PAH composite hydrogel with 15% protein still have the stable swelling ratio at least ninefold.

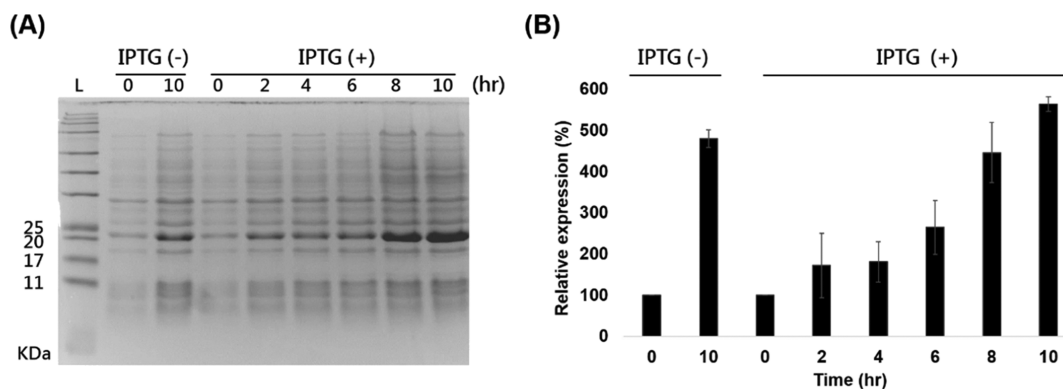


**Figure 2.** (A) Time sequence analysis of SDS-PAGE analysis of IPTG inducing protein expression (L: protein ladder; C0 and C10: protein expression without adding IPTG after 0 and 10 h, respectively; and I0, I2, I4, I6, I8, and I10: protein expression with IPTG after 0, 2, 4, 6, 8, and 10 h). (B) Densitometric analyses. Results are the mean  $\pm$  SD. \* indicates  $p < 0.05$ , compared to the control group ( $n = 4$ ). Abbreviation: IPTG: isopropyl- $\beta$ -D-thiogalactopyranoside.

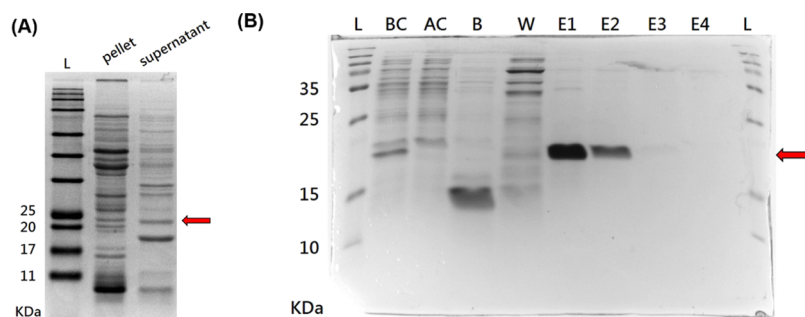


**Figure 3.** (A) SDS-PAGE analysis of the protein contain in the pellet and in supernatant after bacterial disruption. (B) SDS-PAGE analysis of the protein solution produced after column purification ( $n = 4$ ). Abbreviation: L: protein ladder; BC: the protein before passing purification column; AC: the protein after passing purification column; B and W: the protein in binding buffer and wash buffer after passing purification column, respectively; E1, E2, E3, and E4: the first, second, third, and fourth milliliter of elute buffer passed through the purification column, respectively.

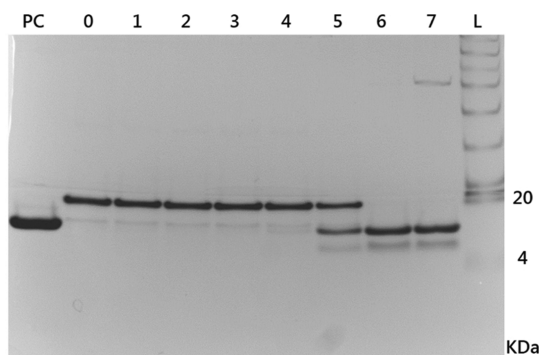


**Figure 4.** SDS-PAGE analysis of the cleavage test ( $n = 4$ ). Abbreviation: L: protein ladder; PC: positive control; and 0–7: the target protein with 0,  $2.5 \times 10^{-6}$ ,  $2.5 \times 10^{-5}$ ,  $2.5 \times 10^{-4}$ ,  $2.5 \times 10^{-3}$ ,  $2.5 \times 10^{-2}$ ,  $2.5 \times 10^{-1}$ , and 2.5 U/mL thrombin, respectively.

**Degradation and Decomposition of the Composite Hydrogel.** Figure 7A shows the schematic diagram of PAH composite hydrogel degradation triggered by the addition of thrombin. Figure 7B shows the degradation ratio of the composite hydrogels by measuring the remaining weight of the hydrogels after incubation with or without thrombin for 72 h. The degradation ratio of the composite hydrogels increased with increasing thrombin-containing protein concentration. When 10 and 15% thrombin-containing proteins were cross-linked with 10% PAH, there was significant differences of the remaining weight in the composite hydrogels by the effect of thrombin-triggered degradation ( $p < 0.05$ ), indicating that the thrombin-containing protein in the composite hydrogel was actually cloven by thrombin in the medium.

Based on the results of swelling and degradation tests, a tube blocked test was established to evaluate the characteristic of the composite hydrogel (Figure 9). The lyophilized composite hydrogel (about 50 mg) was put into a 0.3 cm-diameter tube and then 0.5 cc TBS was added to the tube to swell the gel to block the tube for 1 h. Subsequently, 0.25 unit thrombin was added into the composite hydrogel for 72 h to trigger the gel degradation gradually, making the hydrogel flush out easily. For the sake of safety for future application in the body, the pressure was recorded as  $>15$  kPa to stop the test if the hydrogels could tolerate 15 kPa for 30 s. Table 1 shows that all the pressure was  $>15$  kPa for the PAH alone and the PAH composite hydrogel with 5% protein. One of the tubes with 10% protein composite gel could be opened with pressure 13.1 kPa. Furthermore, all composite hydrogels with 15% protein

could be flushed out with pressure less than 15 kPa. Therefore, we determined the mechanical property of 10P15TP to verify suitable mechanical properties as the nasal-packing material. Figure 8 shows that the compressive modulus and compressive strength of 10P15TP were  $0.28 \pm 0.02$  and  $15.95 \pm 3.11$  kPa, respectively. The experiment successfully confirmed that the composite hydrogels with a higher thrombin-containing protein ratio could be flushed out more easily after being reacted with thrombin.

## DISCUSSION

From the viewpoint of material science, the genetically encoded synthesis provides precise control of molecular weight, sequence, and stereochemistry of repetitive polypeptides. In addition, the recombinant protein in the wake of biotechnology development could be reduced costs.<sup>15,16</sup> Therefore, the artificial protein-based polymers could be credited with desirable chemical, biological, and biocompatible properties to be an alternative to synthetic polymers for biomedical applications.<sup>17</sup> This study combines a non-degradable synthetic PAH polymer and a recombinant protein with a specific enzymatic cleavage site to develop an enzyme-triggered decomposable hydrogel (Figures 6 and 8). The recombinant protein was produced by *E. coli* with the pET-32b(+) plasmid, which is featured with the thioredoxin (Trx) gene containing a thrombin recognition site and with a molecular weight of 20 kDa by SDS-PAGE analysis (Figure 3). Thrombin is a serine proteinase with specificity toward a limited number of substrates<sup>18,19</sup> and is widely used to cleave the protein-purified tag off from the fusion protein.<sup>20–22</sup> Figure 4 shows that the prepared recombinant protein was cleaved into two fragments, 14 and 6 kDa in the presence of  $2.5 \times 10^{-2}$  U/mL thrombin.

Polyelectrolyte hydrogels can be designed to swell or shrink in response to environmental conditions such as pH, temperature, and ion strength.<sup>23</sup> PAH, a typical polyelectrolyte, can be chemically cross-linked with glutaraldehyde to produce a highly swollen hydrogel called a superabsorbent.<sup>24</sup> By blending PAH with protein solution homogeneously, glutaraldehyde would cross-link rapidly the amine groups of PAH and functional groups of proteins<sup>25,26</sup> to form a composite hydrogel (Figure 5). The recombinant protein synthesized in this study was not a superabsorbent material, so it limited the swelling ability of the composite hydrogel. Nevertheless, the composite hydrogel still maintained a high swelling ratio to ninefold when 15% protein was cross-linked with PAH (Figure 6).

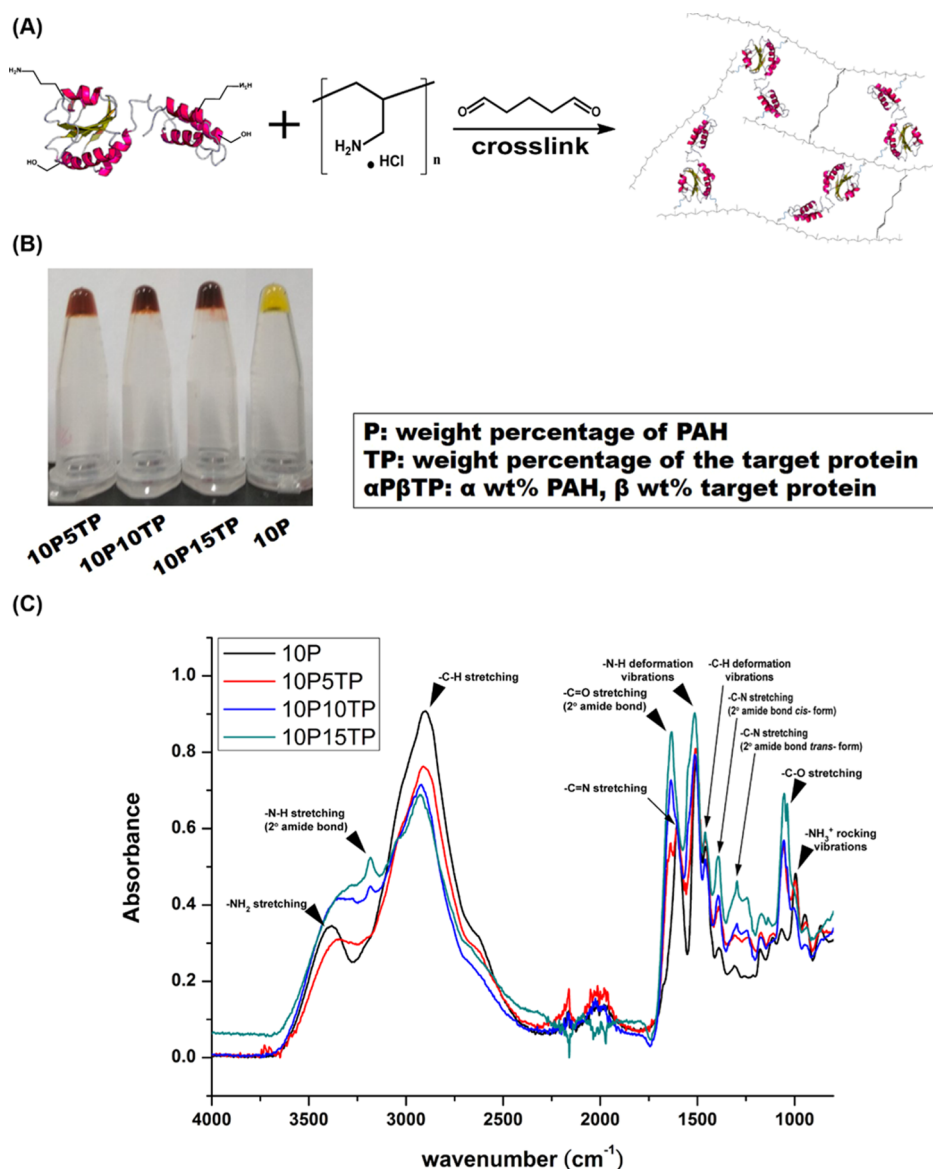


**Figure 5.** (A) Schematic of the cross-link between the target protein and PAH. (B) Inverse test for hydrogel formation. (C) FTIR spectra of PAH composite gel.

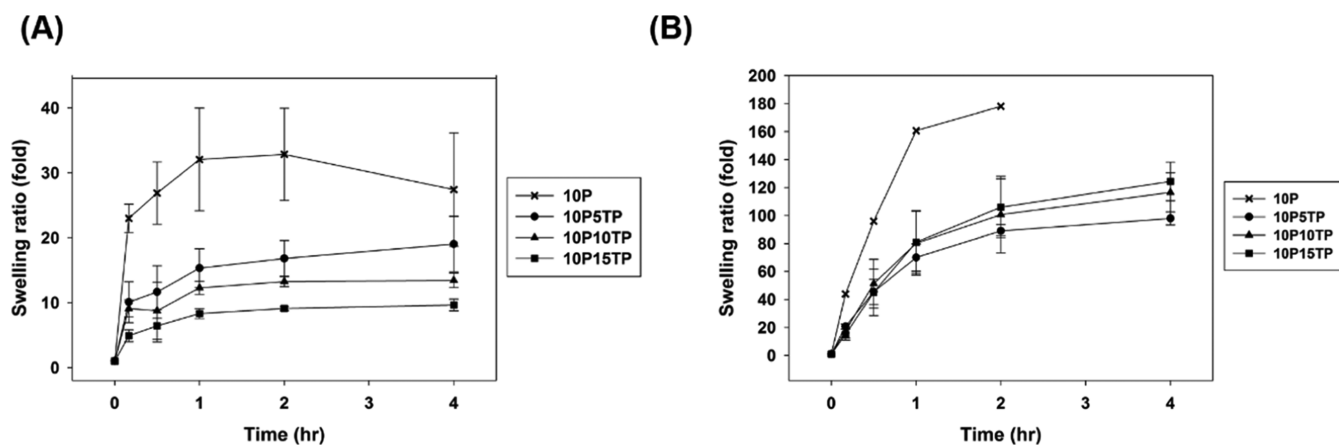


**Figure 6.** Swelling kinetics of the composite hydrogels: (A) in the TBS and (B) in the deionized water ( $n = 6$ ).

Such an enzyme-triggered degradation characteristic possesses the advantage that their structure can be controlled by

protein degradation and then decomposition at an indicated time point, which may be useful in biomedical applications

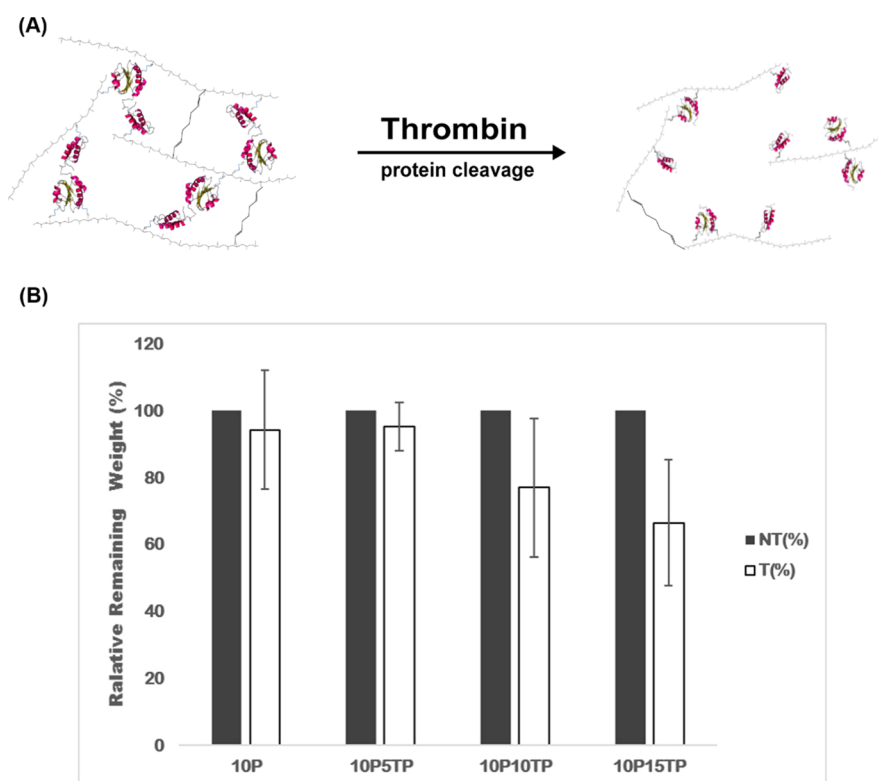


**Figure 7.** (A) Schematic of the mechanism of enzyme-triggered degradation. (B) Degradation ratio of the composite hydrogel degraded with or without thrombin after 72 h ( $n = 4$ ). Abbreviation: T: with thrombin and NT: without thrombin.

**Table 1. Result of the Blocked Tube Test in Unit kPa**

condition	$n = 1$	$n = 2$	$n = 3$	$n = 4$	$n = 5$
10P	×	×	×	×	×
10P5TP	×	×	×	×	×
10P10TP	13.1	×	×	×	×
10P15TP	7.9	14.5	10.3	5.9	3.6

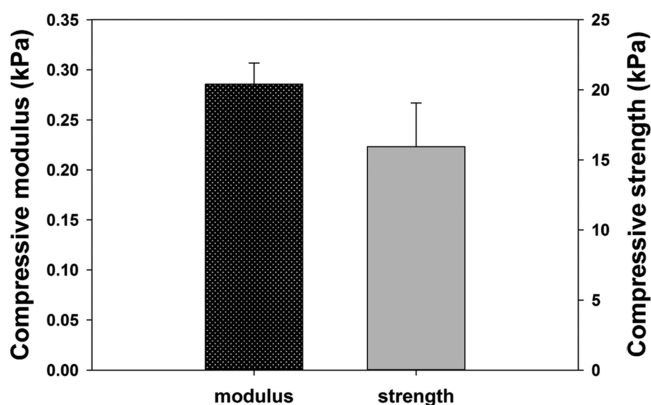


**Figure 8.** Mechanical property of 10P15TP ( $n = 3$ ).

with adequate mechanical properties and controlled biodegradability, such as sinonasal packing materials. For instance, clinically, endoscopic sinus surgery is the preferred treatment for patients with chronic rhinosinusitis that is unresponsive to maximal medical therapy.<sup>27</sup> Biomaterials are generally applied in the sinonasal wound after surgery to achieve hemostasis and prevent postoperative wound synechia. Several studies, by comparing with the degradable and nondegradable nasal packing, indicated that the prolonged nasal packing caused

local irritation, nasal obstruction, discomfort, and pain on removal; nevertheless, degradable packing might improve healing and reduce adhesions, pain, bleeding, nasal blockage, and facial edema.<sup>28,29</sup> Additionally, the ideal biomaterials applied in sinonasal wounds are able to maintain good physical properties initially and then begin to degrade several days after surgery. A single material is difficult to achieve the desired requirements of physical properties and controlled degradation. Figure 7 confirms the enzyme-triggered degradation characteristic of the PAH composite hydrogels. In the absence of thrombin, the composite hydrogel could maintain its weight after incubation for 72 h. Conversely, when the composite hydrogel containing 15% protein was incubated with thrombin, the weight and structure of the PAH composite hydrogel was weakened and unstable and was degraded into fragments. In addition, Figure 8 shows that the mechanical property of the composite hydrogel containing 15% protein was adequately soft for nasal packing. As shown in Figure 9 and Table 1, the tube blocked test revealed that the PAH composite hydrogels were able to swell and block the tube and could be flushed out easily after treatment with thrombin and appropriate pressure less than 15 kPa. Therefore, the PAH composite hydrogels are potentially beneficial to postoperative sinonasal packings since the composite hydrogels not only have adequate physical properties but also can be decomposable by thrombin at the indicated time point.

Gwaltney et al. reported that the maximal pressure of nose blow and sneeze was  $8.8 \pm 1.9$  and  $0.6 \pm 0.5$  kPa, respectively.<sup>30</sup> In addition, the simulation performed by Rahiminejad et al. showed that the pressure in the nasal cavity during normal sneezing was about 1 kPa and suppressing a sneeze by closing nose was about 6 kPa.<sup>31</sup> This study showed that the swollen PAH composite hydrogel could withstand

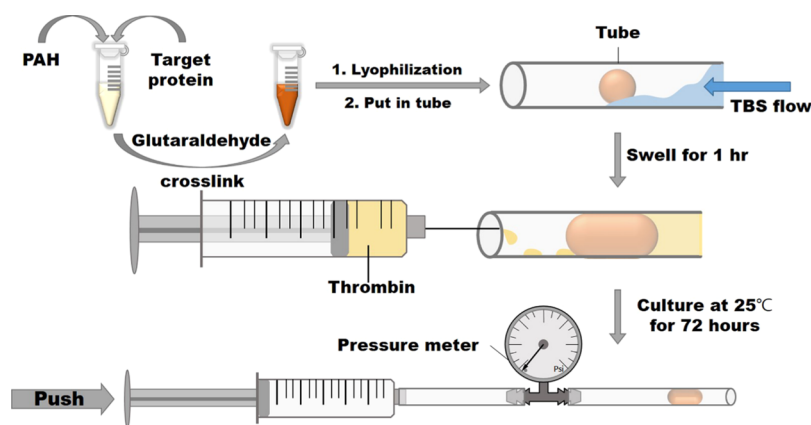


Figure 9. Schematic of the tube blocked test.

more than 15 kPa of pressure in the absence of thrombin. This assured that the PAH composite hydrogel in nasal would not be easily flushed out.

Finally, since the thrombin could decompose the PAH composite hydrogel, the thrombin activity in plasma and hemostasis should be considered. Under normal conditions, the activity of circulation thrombin in plasma is approximately 5.5 mIU/mL.<sup>32</sup> In the process of hemostasis, the activation of thrombin can be regulated by several cytokines, which can not only cause the rising of thrombin concentration but also be rapidly inactive by antithrombin.<sup>33</sup> Therefore, thrombin concentration in plasma is much lower than  $2.5 \times 10^{-2}$  U/mL needed to cleave the prepared recombinant protein (Figure 4). This suggests that the PAH composite hydrogel applied to nasal would not be decomposed by plasma infiltration.

## CONCLUSIONS

In conclusion, using thrombin-containing protein as an example, this study demonstrated that the synthetic super-absorbent polymer, PAH, cross-linked with the recombinant protein with a specific enzymatic cleavage site can be managed by additional thrombin at the indicated time point as a smart biomaterial.

## MATERIALS AND METHODS

**Materials.** All chemicals were purchased from Sigma-Aldrich (St. Louis, MO, USA). The competent cells of *E. coli* ECOS and BL21 (DE3) were purchased from Yeastern Biotech (Taipei, Taiwan) and Agilent Technologies (Santa Clara, CA, USA), respectively. LB broth (Miller) and lysozyme were purchased from BioLink Biotechnology (Taipei, Taiwan). Ampicillin was purchased from MDBio (Taipei, Taiwan). HisTrap used for protein purification was purchased from GE Healthcare (Chicago, IL, USA).

**Plasmids and Bacterial Strains.** The pET-32b(+) vectors (Merck Millipore, USA) carrying a thrombin recognition sequence and T7 promoter system were employed for recombinant protein expression. The ECOS competent *E. coli* cells were transformed with the pET-32b(+) by the heat shock method and stored at  $-80$  °C. The DNA plasmids were extracted using a Presto Mini Plasmid kit (Geneaid, Taiwan) and transformed into the *E. coli* strains BL21 (DE3). *E. coli* cells were cultured in LB broth with 100  $\mu$ g/mL ampicillin at 37 °C and shaken at 180 rpm for 16 h.

**Production of TP.** The transformed *E. coli* strains BL21 (DE3) were incubated in LB broth with 100  $\mu$ g/mL ampicillin at 37 °C and supplemented with 1 mM isopropyl  $\beta$ -D-1-thiogalactopyranoside (IPTG) after the OD600 was within 0.4–0.6 to induce protein production. The optimization of the induction conditions was carried out by measuring the protein content with SDS-PAGE after inducing various lengths of time. After protein induction, the bacterial cultured solution was centrifuged, digested, and ultrasonicated for prepurification. The bacterial cultured solution was centrifuged at 12,000g for 5 min at 4 °C to collect the bacterial pellet. With IB wash buffer (20 mM Tris-HCl pH 7.9, 10 mM EDTA, and 1% Triton X-100) of a one-tenth ratio of the volume of original bacterial suspensions and lysozyme of 100  $\mu$ g per milliliter, the bacterial pellet was suspended and digested in a water bath at 37 °C for 15 min. The ultrasonic disruption of bacterial pellet was carried out with a Cell Disruptor (BRANSON, USA). After centrifugation at 12,000g for 5 min at 4 °C, the supernatant was collected to dialyze in 20 mM Tris-HCl solution and then to filter with 0.45  $\mu$ m filters.

A HisTrap FF column was used for TP purification. In brief, using a syringe pump with a flow rate of 1 mL per minute to load protein solution onto a column which had been washed by distilled water and equilibrated by binding buffer, the column was washed again and eluted with the Tris-HCl buffer supplemented with 20 and 500 mM imidazole, respectively. The eluted protein was collected and changed into 20 mM Tris-HCl buffer through ultrafiltration with an Amicon Ultra-4 Centrifugal Filter (Merck Millipore, USA). The purified TP was directly freeze-dried for further use.

TP characterization was carried out with 12% sodium dodecyl sulfate polyacrylamide gel electrophoresis (SDS-PAGE). The sample protein was mixed with 2 $\times$  Laemmli sample buffer (Bio-Rad, Hercules, CA, USA) and heated at 90 °C for 5 min before loading. The gel was stained by coomassie brilliant blue solution (40% methanol, 10% acetic acid, and 0.1% coomassie brilliant blue R-250) for 2 h and destained in 50% methanol solution. The gel was scanned and imaged using a BioSpectrum 810 Imaging System (UVP, Upland, CA, USA).

**Thrombin Cleavage Test.** The thrombin cleavage test was conducted according to the procedure of the thrombin kit. TP was dissolved in the thrombin cleavage buffer containing 20 mM Tris-HCl, 150 mM NaCl, and 2.5 mM  $\text{CaCl}_2$  to prepare 20 mg/mL solution. A series of thrombin concentration was added into TP solution and incubated at room temperature for

16 h. The SDS-PAGE analysis was carried out to find out the optimal thrombin cleavage concentration.

**Synthesis of Target Protein–Poly(allylamine hydrochloride) Composite Hydrogels.** A series of composite hydrogels were synthesized from cross-linking target protein and PAH with 1% glutaraldehyde. Glutaraldehyde could fast and efficiently cross-link poly(allylamine hydrochloride) into hydrogels by the reaction between amines and aldehyde group. In addition, glutaraldehyde could react with the amino groups of amino acids and partially react with the phenolic and the imidazole rings of tyrosine and histidine derivatives in proteins.

The stock solutions were prepared by dissolving 0.3 g of target protein in 0.7 mL of deionized water and 0.4 g of PAH in 0.6 mL of deionized water, respectively. The resulting solution was prepared by blending a consistent amount of PAH stock solution with various amounts of target protein stock solution. Cross-linked with 1% glutaraldehyde and mixed homogeneously with the vortex immediately, the composite hydrogels were prepared after being reacted at room temperature for 24 h.

**Degradation Test.** The remaining percentage is expressed as the weight ratio of hydrogels reacted with thrombin for 72 h to the one before being reacted. The freeze-dried composite hydrogels were weighed and immersed in thrombin cleavage buffer which is mentioned in the thrombin cleavage test. To make sure that the thrombin reacted completely, 2.5 units of thrombin per milliliter which is overdose thrombin concentration was added to the hydrogel contained solution. After being incubated at room temperature for 72 h, hydrogels were taken out from solutions, freeze-dried, and weighted to calculate the remaining percentage.

**Swelling Test.** The swelling ratio is expressed as the weight ratio of swollen hydrogels to the initial freeze-dried hydrogels, swelling ratio =  $W_{\text{wet}}/W_{\text{dry}}$ . Hydrogels were weighted, put in vials, and weighted again as the initial condition. TBS buffer and deionized water were added into the vials, respectively. At the scheduled time points, the solution was removed from the vials and weighted to calculate the swelling ratio. After being weighted, TBS buffer and deionized water were added back into the vials.

**Blocked Tube Test.** Figure 9 shows the procedure for a blocked tube test. First of all, freeze-dried composite hydrogels were placed inside tubes. Flowed with TBS buffer in tubes for 1 h, the composite hydrogels would swell and block the tubes. The thrombin cleavage buffer mentioned in the thrombin cleavage test with 2.5 units of thrombin per milliliter was prepared and it replaced the TBS buffer solution in tubes. After being incubated at room temperature for 72 h, the max pressure the hydrogel could resist is measured with the equipment, as shown in Figure 9.

**Mechanical Property Test.** The composite hydrogels were prepared in regular shapes with a diameter of 3.35 mm, and the height of each composite hydrogel was measured directly with an MTS Landmark dynamic test system. The composite hydrogels were compressed with a rate of 0.01 mm/s unit mechanical failure. The compressive modulus of the composite hydrogel was calculated by fitting the initial slope of the stress–strain curves.

**Statistical Analysis.** Each experiment was performed in triplicate to sextuplicate, and all data examined were expressed as the mean  $\pm$  standard deviation. Comparative analysis of two groups was conducted using the Student's *t*-test. Differences between multiple groups were compared using one-way

analysis of variance (ANOVA) followed by the Bonferroni test. A *p* value <0.05 indicated a significant difference.

## ■ ASSOCIATED CONTENT

### Supporting Information

The Supporting Information is available free of charge at <https://pubs.acs.org/doi/10.1021/acsomega.1c05178>.

FTIR spectra of PAH polymer and PAH gel (10P) (PDF)

## ■ AUTHOR INFORMATION

### Corresponding Authors

**Shyr-Yi Lin** – Division of Gastroenterology, Department of Internal Medicine, Wan Fang Hospital, Taipei Medical University, Taipei 116, Taiwan; Department of General Medicine, School of Medicine, College of Medicine, Taipei Medical University, Taipei 110, Taiwan; Email: [sylin@tmu.edu.tw](mailto:sylin@tmu.edu.tw)

**Tsung-Wei Huang** – Department of Electrical Engineering, College of Electrical and Communication Engineering, Yuan Ze University, Taoyuan 320, Taiwan; Department of Otolaryngology, Far Eastern Memorial Hospital, New Taipei City 220, Taiwan; Email: [huangtw28@gmail.com](mailto:huangtw28@gmail.com)

**Tai-Hong Young** – Institute of Biomedical Engineering, College of Medicine and College of Engineering, National Taiwan University, Taipei 100, Taiwan; Department of Biomedical Engineering, National Taiwan University Hospital, Taipei 100, Taiwan; [orcid.org/0000-0001-5338-4747](https://orcid.org/0000-0001-5338-4747); Email: [thyong@ntu.edu.tw](mailto:thyong@ntu.edu.tw)

### Authors

**You-Ren Ji** – Institute of Biomedical Engineering, College of Medicine and College of Engineering, National Taiwan University, Taipei 100, Taiwan; [orcid.org/0000-0001-6394-041X](https://orcid.org/0000-0001-6394-041X)

**Ya-Hsiang Hsu** – Institute of Biomedical Engineering, College of Medicine and College of Engineering, National Taiwan University, Taipei 100, Taiwan

**Ming-Hua Syue** – Institute of Biomedical Engineering, College of Medicine and College of Engineering, National Taiwan University, Taipei 100, Taiwan

**Ying-Chu Wang** – Institute of Biomedical Engineering, College of Medicine and College of Engineering, National Taiwan University, Taipei 100, Taiwan

Complete contact information is available at:

<https://pubs.acs.org/10.1021/acsomega.1c05178>

### Author Contributions

<sup>†</sup>They contributed equally to this work.

### Notes

The authors declare no competing financial interest.

## ■ ACKNOWLEDGMENTS

The authors thank the Ministry of Science and Technology, Taiwan, for their financial support (108-2314-B-002-104-MY3).

## ■ REFERENCES

(1) Collier, J. H.; Segura, T. Evolving the Use of Peptides as Components of Biomaterials. *Biomaterials* **2011**, *32*, 4198–4204.

- (2) Balint, R.; Cassidy, N. J.; Cartmell, S. H. Conductive Polymers: Towards a Smart Biomaterial for Tissue Engineering. *Acta Biomater.* **2014**, *10*, 2341–2353.
- (3) Nair, L. S.; Laurencin, C. T. Polymers as Biomaterials for Tissue Engineering and Controlled Drug Delivery. *Adv. Biochem. Eng./Biotechnol.* **2006**, *102*, 47–90.
- (4) Huang, T.-W.; Chan, Y.-H.; Su, H.-W.; Chou, Y.-S.; Young, T.-H. Increased Mucociliary Differentiation and Aquaporins Formation of Respiratory Epithelial Cells on Retinoic Acid-loaded Hyaluronan-derivative Membranes. *Acta Biomater.* **2013**, *9*, 6783–6789.
- (5) Huang, T.-W.; Li, S.-T.; Young, T.-H. Chitosan-hyaluronan: Promotion of Mucociliary Differentiation of Respiratory Epithelial Cells and Development of Olfactory Receptor Neurons. *Artif. Cells, Nanomed., Biotechnol.* **2019**, *47*, 564–570.
- (6) Nair, L. S.; Laurencin, C. T. Biodegradable Polymers as Biomaterials. *Prog. Polym. Sci.* **2007**, *32*, 762–798.
- (7) Hubbell, J. A. Biomaterials in Tissue Engineering. *Nat. Biotechnol.* **1995**, *13*, 565–576.
- (8) Azevedo, H. S.; Gama, F. M.; Reis, R. L. In vitro Assessment of the Enzymatic Degradation of Several Starch Based Biomaterials. *Biomacromolecules* **2003**, *4*, 1703–1712.
- (9) Hubbell, J. Bioactive Biomaterials. *Curr. Opin. Biotechnol.* **1999**, *10*, 123–129.
- (10) Chertow, G. M.; Burke, S. K.; Michael Lazarus, J.; Stenzel, K. H.; Wombolt, D.; Goldberg, D.; Bonventre, J. V.; Slatopolsky, E. Poly[allylamine hydrochloride] (RenaGel): a Noncalcemic Phosphate Binder for the Treatment of Hyperphosphatemia in Chronic Renal Failure. *Am. J. Kidney Dis.* **1997**, *29*, 66–71.
- (11) Vinogradova, O. I.; Lebedeva, O. V.; Vasilev, K.; Gong, H.; Garcia-Turiel, J.; Kim, B.-S. Multilayer DNA/Poly(allylamine hydrochloride) Microcapsules: Assembly and Mechanical Properties. *Biomacromolecules* **2005**, *6*, 1495–1502.
- (12) Kreke, M. R.; Badami, A. S.; Brady, J. B.; Michael Akers, R.; Goldstein, A. S. Modulation of Protein Adsorption and Cell Adhesion by Poly(allylamine hydrochloride) Heparin Films. *Biomaterials* **2005**, *26*, 2975–2981.
- (13) Yoshimura, T.; Matsuo, K.; Fujioka, R. Novel Biodegradable Superabsorbent Hydrogels Derived from Cotton Cellulose and Succinic Anhydride: Synthesis and Characterization. *J. Appl. Polym. Sci.* **2006**, *99*, 3251–3256.
- (14) LaVallie, E. R.; DiBlasio, E. A.; Kovacic, S.; Grant, K. L.; Schendel, P. F.; McCoy, J. M. A Thioredoxin Gene Fusion Expression System that Circumvents Inclusion Body Formation in the E. coli Cytoplasm. *Nat. Biotechnol.* **1993**, *11*, 187–193.
- (15) Kesik-Brodacka, M. Progress in biopharmaceutical development. *Biotechnol. Appl. Biochem.* **2018**, *65*, 306–322.
- (16) Chen, Q.; Lai, H. Gene delivery into plant cells for recombinant protein production. *BioMed Res. Int.* **2015**, *2015*, 1–10.
- (17) MacEwan, S. R.; Chilkoti, A. Elastin-like Polypeptides: Biomedical Applications of Tunable Biopolymers. *Biopolymers* **2010**, *94*, 60–77.
- (18) Berliner, L. J. *Thrombin: Structure and Function*, 1st ed.; Berliner, L. J., Ed.; Plenum Press: New York, 2012; pp 1–438.
- (19) Wells, C. M.; Di Cera, E. Thrombin is a sodium ion activated enzyme. *Biochemistry* **1992**, *31*, 11721–11730.
- (20) Meyer, D. E.; Chilkoti, A. Purification of Recombinant Proteins by Fusion with Thermally-Responsive Polypeptides. *Nat. Biotechnol.* **1999**, *17*, 1112–1115.
- (21) Jenny, R. J.; Mann, K. G.; Lundblad, R. L. A Critical Review of the Methods for Cleavage of Fusion Proteins with Thrombin and Factor Xa. *Protein Expression Purif.* **2003**, *31*, 1–11.
- (22) CHANG, J.-Y. Thrombin specificity. Requirement for apolar amino acids adjacent to the thrombin cleavage site of polypeptide substrate. *Eur. J. Biochem.* **1985**, *151*, 217–224.
- (23) Qiu, Y.; Park, K. Environment-sensitive Hydrogels for Drug Delivery. *Adv. Drug Delivery Rev.* **2012**, *64*, 49–60.
- (24) Bui, T. Q.; Cao, V. D.; Do, N. B. D.; Christoffersen, T. E.; Wang, W.; Kjoniksen, A.-L. Salinity Gradient Energy from Expansion and Contraction of Poly(allylamine hydrochloride) Hydrogels. *ACS Appl. Mater. Interfaces* **2018**, *10*, 22218–22225.
- (25) Tong, W.; Gao, C.; Möhwald, H. Single Polyelectrolyte Microcapsules Fabricated By Glutaraldehyde-Mediated Covalent Layer-By-Layer Assembly. *Macromol. Rapid Commun.* **2006**, *27*, 2078–2083.
- (26) Habeeb, A. F. S. A.; Hiramoto, R. Reaction of Proteins with Glutaraldehyde. *Arch. Biochem. Biophys.* **1968**, *126*, 16–26.
- (27) Wormald, P. *Endoscopic Sinus Surgery: Anatomy, Three-Dimensional Reconstruction, and Surgical Technique*, 3rd ed.; Wormald, P., Ed.; Thieme Medical Publishers: New York, 2012; pp 1–304.
- (28) Berlucchi, M.; Castelnuovo, P.; Vincenzi, A.; Morra, B.; Pasquini, E. Endoscopic Outcomes of Resorbable Nasal Packing after Functional Endoscopic Sinus Surgery: A Multicenter Prospective Randomized Controlled Study. *Arch. Oto-Rhino-Laryngol.* **2009**, *266*, 839–845.
- (29) Verim, A.; Şeneldir, L.; Naiboğlu, B.; Karaca, Ç. T.; Külekçi, S.; Toros, S. Z.; Oysu, Ç. Role of Nasal Packing in Surgical Outcome for Chronic Rhinosinusitis with Polyposis. *Laryngoscope* **2014**, *124*, 1529–1535.
- (30) Gwaltney, J. M.; Hendley, J. O.; Phillips, C. D.; Bass, C. R.; Mygind, N.; Winther, B. Nose Blowing Propels Nasal Fluid into the Paranasal Sinuses. *Clin. Infect. Dis.* **2000**, *30*, 387–391.
- (31) Rahiminejad, M.; Haghghi, A.; Dastan, A.; Abouali, O.; Farid, M.; Ahmadi, G. Computer Simulations of Pressure and Velocity Fields in a Human Upper Airway During Sneezing. *Comput. Biol. Med.* **2016**, *71*, 115–127.
- (32) Stief, T. W. Specific Determination of Plasmatic Thrombin Activity. *Clin. Appl. Thromb./Hemostasis* **2006**, *12*, 324–329.
- (33) Bock, S. C. Antithrombin III Genetics, Structure and Function. In *Recombinant Technology in Hemostasis and Thrombosis*, 1st ed.; Drohan, W. N., Hoyer, L. W., Eds.; Plenum Press: New York 1991; pp 25–45.